IEEE TRANSACTIONS ON ELECTRON DEVICES, VOL. 65, NO. 9, SEPTEMBER 2018

Simple and Fast Approach for Synthesis of Reduced Graphene Oxide–MoS_2 Hybrids for Room Temperature Gas Detection

Rajesh Kumar, Wagner Dias, Jr., Rafael J. G. Rubira, Andrei V. Alaferdov, Alfredo R. Vaz,
Rajesh K. Singh, Silvio R. Teixeira, Carlos J. L. Constantino,
and Stanislav A. Moshkalev, *Member, IEEE*

***Abstract*— The combination of two highly versatile materials as reduced graphene oxide (rGO) and molybdenum disulfide (MoS_2) forms the layered rGO–MoS_2 hybrids that have great potential for sensing applications. In this paper, we developed a cost-effective, time-saving, and efficient microwave-assisted method to exfoliate rGO and MoS_2 nanosheets in a powder mixture for the formation of rGO–MoS_2 hybrids. The formation of hybrids with a combination of organic and inorganic 2-D layered materials offers new possibilities for the development of gas sensitive materials. The applied microwave treatment is a simple and fast process for the large-scale synthesis of rGO–MoS_2 hybrids. The synthesized rGO–MoS_2 hybrids were characterized by X-ray diffraction, scanning electron microscope, energy dispersive X-ray spectroscopy, Raman, X-ray photoelectron spectroscopy, and thermogravimetric analyses to determine the phase structure, surface morphology, defect formation, binding energy, thermal stability and so on. The synthesized rGO–MoS_2 hybrids were tested for sensing application and showed the good performance to detect gases such as O_2, N_2, and NH_3 at room temperature.**

***Index Terms*— 2-D layered materials, characterization, gas sensor, hybrids, microwave exfoliation, molybdenum disulfide (MoS_2), reduced graphene oxide (rGO).**

I. INTRODUCTION

THE discovery of 2-D graphene and its excellent properties has encouraged numerous studies for various kinds of applications. Also, the derivatives of graphene, such as graphene oxide (GO) and reduced GO (rGO), have recently concerned remarkable research curiosity owing to their unique structural and outstanding electronic, mechanical, and thermal properties. The GO/rGO layers contain different functional groups such as hydroxyl and epoxy groups on sp^3 hybridized carbon on the basal plane, in addition to carbonyl and carboxyl groups located at the sheet edges on sp^2 region [1]. These oxygen-containing functional groups attached to GO/rGO makes it more sensitive, and its degree of sensitivity depends on these attached functional groups [2]. Due to nearly absence of bandgap in graphene and its derivatives, there are numerous efforts to find out other types of 2-D layered inorganic materials such as transition metal dichalcogenides (TMDs). In the category of TMDs, molybdenum disulfide (MoS_2) contains graphene-liked 2-D layered n-type semiconductor, which composed of three atom layers (S–Mo–S) and also stacked through a weak Van der Waals force [3]. These MoS_2 layered materials have stimulated intensive research due to their outstanding semiconducting nature with unique thickness-dependent physical properties which are used for versatile electronic, optical, and sensing applications.

Several research studies on rGO-based gas sensors are discussed and show the potential of rGO in sensing application [4]–[6]. The rGO-based sensors are capable of detection of chemically aggressive gases, such as NO_2, NH_3, Cl_2, and NO with the typical response and recovery times of about several tens of minutes [4], [7]–[10]. Also, the assembled structure graphene into a 3-D graphene aerogel may open up new prospects for improved sensing properties by maintaining a high surface area in a porous network [11]–[13]. However, graphene and its derivatives-based sensors show a poor selectivity without proper surface modification [10], [14]–[17]. Therefore, it is remarkably important to develop high performance containing gas sensors that are capable of sensing low concentrations of gases in atmosphere precisely, constantly, and rapidly for human health safety

---

Manuscript received May 11, 2018; revised June 22, 2018; accepted June 27, 2018. Date of publication July 19, 2018; date of current version August 21, 2018. This work was supported in part by FAPESP (2013/14262-7 and 2017/22186-0) and in part by CNPq, Brazil. The review of this paper was arranged by Editor F. Schwierz. *(Corresponding authors: Rajesh Kumar; Stanislav A. Moshkalev.)*

R. Kumar was with the Centre for Semiconductor Components and Nanotechnology, University of Campinas, Campinas 13083-870, Brazil. He is now with the Faculty of Science and Technology, Department of Physics, São Paulo State University, Presidente Prudente 19060-900, Brazil (e-mail: rajeshbhu1@gmail.com).

W. Dias, Jr., R. J. G. Rubira, S. R. Teixeira, and C. J. L. Constantino are with the Faculty of Science and Technology, Department of Physics, São Paulo State University, Presidente Prudente 19060-900, Brazil (e-mail: snow_dias@hotmail.com; rafael.gon.fis@gmail.com; rainho@fct.unesp.br; carlos.constantino@unesp.br).

A. V. Alaferdov, A. R. Vaz, and S. A. Moshkalev are with the Centre for Semiconductor Components and Nanotechnology, University of Campinas, Campinas 13083-870, Brazil (e-mail: analaferdov@gmail.com; alfredo@ccs.unicamp.br; stanisla@unicamp.br).

R. K. Singh is with the School of Physical and Material Sciences, Central University of Himachal Pradesh, Dharamshala HP-176215, India (e-mail: rksbhu@gmail.com).

Color versions of one or more of the figures in this paper are available online at http://ieeexplore.ieee.org.

Digital Object Identifier 10.1109/TED.2018.2851955

and air-quality monitoring [18]. The single-/few-layered MoS_2 shows improved selectivity compared to graphene, makes an exciting candidate for gas sensing application including at a room temperature. Single/few layers synthesized MoS_2 has been used as a prospective sensing material for several kinds of gases [3], [18]–[25]. The MoS_2-based field-effect transistor sensors have slow response and recovery times or even no recovery when used at normal room temperature [26]–[31].

Graphene with single-/few-layer MoS_2 nanosheets (MoS_2 NSs) reveals enhanced excellent properties and offers the possibilities to create new kinds of devices for daily human life such as supercapacitors, lithium storage, and DNA sensing [32]–[37]. The combined structure of graphene/rGO with MoS_2 shows a good application for gas sensing. For conductometric sensing purposes, the graphene derivatives allow for lower noise measurements than MoS_2 alone, since MoS_2 is much less conductive than graphene due to its semiconducting nature [37]. The 2-D structure of the MoS_2 on graphene/rGO increases the contact area for efficient charge transfer across the interface and shortens the charge transport time and distance, which improve the device performance [35], [36], [38]. Also, the formation of hybrids with the combination of graphene/rGO–MoS_2 architectures can improve their electrochemical, catalytic, and sensing behaviors [33], [39]. Niu *et al.* [3] have reported the synthesis of rGO/MoS_2 composite using two-step process (wet spinning and hydrothermal) for NO_2 and NH_3 gas sensing. Cho *et al.* [40] have developed atomically thin heterostructure-based gas sensor via the combination of MoS_2 (mechanically exfoliated) and graphene (synthesized via chemical vapor deposition) for the detection of NO_2 gas.

In this paper, we have developed one-step, simple, rapid, and large-scale synthesis using microwave-assisted rGO–MoS_2 hybrids for application at room temperature gas (O_2, N_2, and NH_3) sensors. The fast chemical reactions on rGO–MoS_2 hybrids surfaces using this method enable reducing production costs and enhancing sensing capabilities. These studies revealed the potential application of rGO–MoS_2 hybrids for a different gas sensing.

II. EXPERIMENTS

A. Synthesis of rGO Nanosheets

Graphite oxide was synthesized by the chemical oxidation of graphite powder, using the modified Staudenmaier's method [41], [42]. Graphite powder (5 g) was continuously stirred with a combination of sulfuric acid (90 mL) and nitric acid (45 mL) solution at room temperature. The solution container was placed into an ice water bath to make sure constant temperature and subsequently, potassium chlorate ($KClO_3$) (40 g) was gradually poured into the solution to reduce the risk of explosion due to the exothermic reaction. This solution was kept for 6 days under continuous magnetic stirring at room temperature for superior oxidation of the graphite powder. The as-obtained graphite oxide product was washed with deionized water (DI) water and further 10% hydrochloric solution was added to eliminate sulfate and other ion impurities. It was then again washed several times with DI water until a pH of 7 was reached. Afterward, the graphite oxide powder was dried at 60 °C under vacuum for complete dry. The dried graphite oxide powder was directly irradiated (700 W and 70 s) in a domestic microwave oven (Consul-CMW30AB, 1-kW total power) for reduction and exfoliation into rGO.

B. Synthesis of rGO–MoS_2 Hybrids

The graphite oxide suspension was obtained by mixing 100 mg of graphite oxide powder in 120 mL of C_2H_5OH assisted with continuous magnetic stirring (20 min) and sonication. To prepare the rGO–MoS_2 hybrids, MoS_2 powder (50 mg) was added into the as-prepared graphite oxide suspension under continuous stirring for 20 min. Finally, the prepared solution was dried in open atmosphere for complete evaporation of C_2H_5OH and dried powder was treated with microwave (Consul-CMW30AB) irradiation (800 W and 130 s) for complete exfoliation and reduction graphite oxide into rGO with MoS_2 powder for the final formation of rGO–MoS_2 hybrids.

C. Characterization

The structural characterization of the synthesized rGO–MoS_2 hybrids was performed by X-ray diffraction (XRD—D/MAX-2500/PC; Rigaku Corporation, Tokyo, Japan) over the 2θ range 5°–75°. The surface morphology and elemental analysis were investigated using scanning electron microscope (SEM—dual beam focused ion beam/field emission gun model FEI Nova 200) equipped with energy dispersive X-ray spectroscopy (EDS). Raman measurements were carried out to determine the defect inside the material using a spectrometer with a 473-nm laser (NT-MDT NTEGRA spectra). X-ray photoelectron spectroscopy (XPS) measurements were performed using a SPECS system XR 50 X-ray source (Al Kα, 1486.6 eV) equipped Phoibos 150 hemispherical energy analyzer with MCD-9 detector. Thermogravimetric measurements were carried out with an SDT Q600 thermogravimetric analyses (TGAs) apparatus (TA Instruments, New Castle, DE, USA), and the samples were heated at a rate of 10 °C/min from room temperature to 850 °C at air flow (100 mL/min) atmosphere.

D. Gas Sensing Measurements

The gas sensing tests were carried out in a vacuum chamber at room temperature. In the fabrication process, the as-prepared rGO–MoS_2 hybrid powder was used for the preparation of two types of resistive gas sensors. First, a thick-film sensitive element was prepared in the form of a disk with a diameter of 10 mm and a thickness of 2 mm, with two parallel metal electrodes fixed in the opposite parts of the disk with the spacing between the electrodes about 8 mm. The electrodes were prepared using copper wires with diameters of 0.05 mm covered with gold. The powder together with electrodes was pressed to form disks with a density of 1.8 g/cm^3. The resistance of the material between electrodes was measured to be near 20 Ω and its resistivity near 4 $\Omega \cdot$ cm. Second, a thin-film sensor was prepared by drop casting of isopropyl alcohol solution containing the powder between two parallel thin-film graphite electrodes (width of 10 mm, the gap between

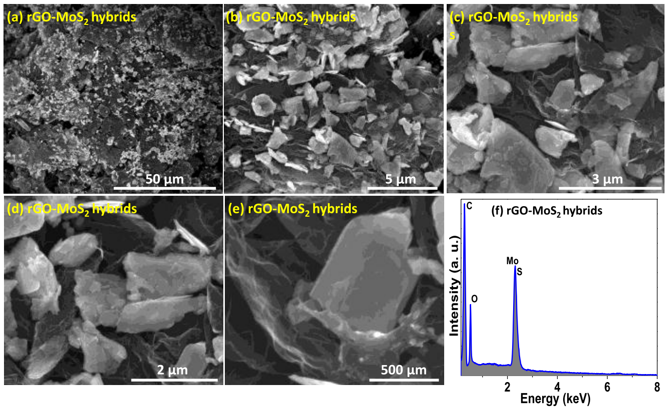

Fig. 1. (a)–(e) SEM rGO–MoS_2 hybrids at different magnifications. (f) EDS of rGO–MoS_2 hybrids.

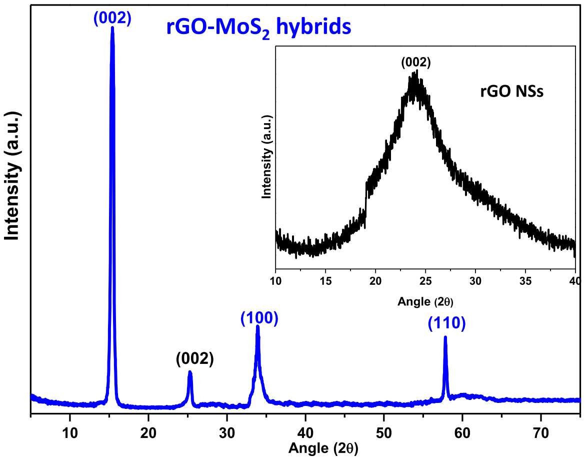

Fig. 2. XRD of rGO NSs and rGO–MoS_2 hybrids.

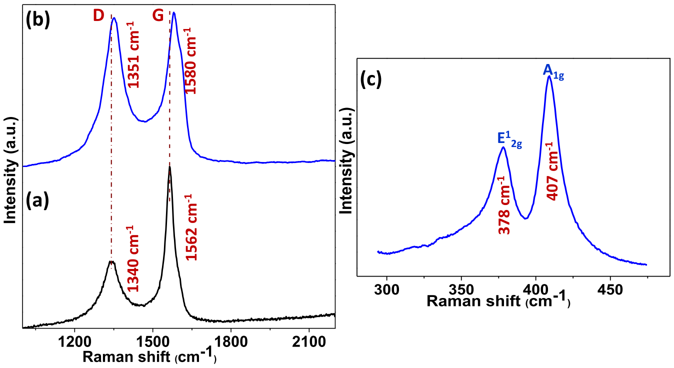

Fig. 3. Raman spectra of (a) rGO NSs and (b) and (c) rGO–MoS_2 hybrids.

electrodes 1 mm) formed over a flexible polydimethylsiloxane support using the Langmuir–Blodgett method [43]. An estimated average thickness of the rGO–MoS_2 layer after drying was near 0.01 mm, and the sensor resistance was measured to be 10 kΩ. The prepared sensing elements were placed in a vacuum chamber with a base pressure of 10^{-5} mbar. The current through the sensors was maintained at 1 mA, and the voltage drops between two electrodes were measured. The sensors were exposed to different gases as N_2, O_2, and NH_3 vapor at room temperature.

III. RESULTS AND DISCUSSION

The surface morphology of the rGO–MoS_2 hybrids was characterized using SEM. SEM micrographs of the as-synthesized rGO–MoS_2 hybrids (Fig. 1) show that the synthesized materials assembled with the homogeneous distribution of rGO and MoS_2 in the hybrids. The rGO, NSs, and MoS_2 NSs are interconnected to each other. Specially, the porous morphology of rGO NSs gives the good supports for MoS_2 NSs and it can be clearly seen in Fig. 1(e), which facilitates gas diffusion during the sensing application. The surface analysis indicates that most of the rGO NSs are covered by MoS_2 NSs. The uniform distribution of MoS_2 NSs on the rGO NSs is confirmed by EDS as shown in Fig. 1(f), where C, O, Mo, and S are seen to be uniformly distributed throughout the rGO–MoS_2 hybrids.

To determine the structural analysis, XRD patterns of the synthesized rGO NSs and rGO–MoS_2 hybrids are shown in Fig. 2. The inset of the figure shows the XRD pattern of rGO NSs, which was exfoliated and reduced by microwave irradiation. The three sharp diffraction peaks of rGO–MoS_2 hybrids center at around $2\theta = 15.1°$, $33.8°$, and $57.5°$ corresponding to the (002), (100), and (110) planes, respectively, for MoS_2. These all of the diffraction peaks can be well indexed to the hexagonal phase of MoS_2 (Joint Committee on Powder Diffraction Standards No. 37-1492) [3], [44]. The small and broad diffraction peak of rGO NSs at $2\theta = 25.2°$ corresponding to (002) plane can be seen in the rGO–MoS_2 hybrids, suggesting the presence of rGO NSs in hybrids.

Raman spectroscopy is a powerful tool for the characterization of rGO and others 2-D layered materials [45], [46]. The Raman spectra of the as-synthesized rGO NSs and rGO–MoS_2 hybrids are shown in Fig. 3. The two dominant peaks in Raman spectrum show a typical *D*-band and *G*-band for graphene and its derivatives (rGO NSs), which present the defects or structural disorders (sp^3) and tangential vibration of carbon atoms (sp^2), respectively, [47], [48]. The *D*-band and *G*-band observed in rGO appear at 1340 and 1562 cm^{-1}, respectively, [Fig. 3(a)]. After formation of rGO–MoS_2 hybrids, the *D*-band and *G*-band of the rGO–MoS_2 hybrids observed at 1351 and 1580 cm^{-1}, respectively, [Fig. 3(b)]. These significant shiftings were observed in the *G*-band positions in rGO–MoS_2 hybrids because of the interaction of MoS_2. Furthermore, the broadening of Raman peaks (*D*-band and *G*-band) for rGO–MoS_2 hybrids are the witnessed for the existence of MoS_2. Also, the I_D/I_G ratio can be used for the indication of the rGO–MoS_2 hybrids quality. The relative intensity of I_D/I_G was around 0.96 in rGO–MoS_2 hybrids is much higher than that in pristine rGO NSs (0.41), revealing that some defects and disordered structures such as wrinkles, holes, charged impurities, and others can be introduced on the surface of rGO due to the addition of MoS_2. This phenomenon is supposed to be attributed to the electron transfer between rGO and MoS_2. The lower wavenumber part of Raman spectra of rGO–MoS_2 hybrids reveals the well-known characteristic peaks of MoS_2 [Fig. 3(c)]. The major peaks associated with

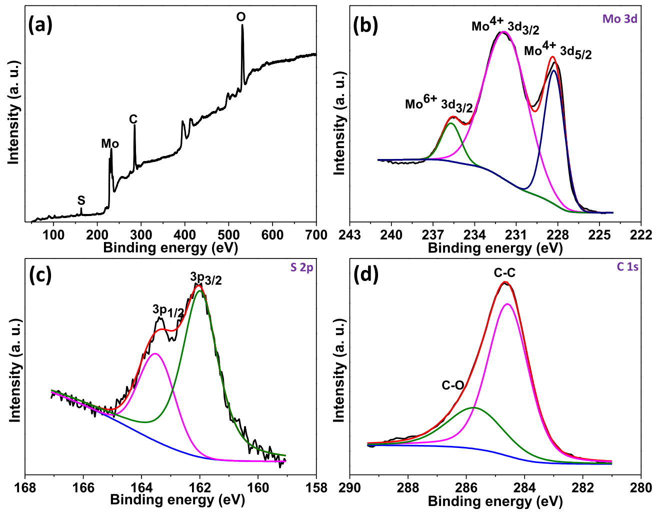

Fig. 4. XPS spectra of rGO–MoS_2 hybrids. (a) Complete survey, (b) Mo 3d, (c) S 2p, and (d) C1s peaks.

MoS_2 are at 378 and 407 cm^{-1} and correspond to the in-plane E^1_{2g} and out-of-plane A_{1g} vibrational modes of hexagonal MoS_2, respectively, in a good agreement with the literature values for multilayer MoS_2 [3], [18], [49]. The E^1_{2g} mode involves the in-layer relative displacement between Mo and S atoms, while the A_{1g} mode involves the out-of-layer vertical-vibration displacements of S atoms along the *c*-axis.

XPS is used to further study the surface electronic state of rGO–MoS_2 hybrids. The chemical composition of rGO–MoS_2 hybrids samples is characterized by XPS spectra. Sulfur, molybdenum, carbon, and oxygen peaks are clearly identified in the survey spectrum in Fig. 4(a). The high-resolution scan for Mo 3d, S 2p, C1s, and O1s has been shown in Fig. 4(b)–(d). The Mo peaks show two Mo oxidation states (Mo^{4+} and Mo^{6+}), which can be indexed to the Mo–S and the Mo–O bonding, respectively. The Mo 3d spectra show two Mo oxidation states (Mo^{4+} and Mo^{6+}). The Mo 3d clearly shows three peaks at 228.3, 231.9, and 235.1 eV [Fig. 4(b)]. The first two peaks (228.3 and 231.9 eV) are attributed to the doublet Mo $3d_{5/2}$ and Mo $3d_{3/2}$, respectively, correlating to Mo^{4+} state in MoS_2(typical of the Mo–S bond). The third peak of Mo $3d_{5/2}$ at 235.1 eV is attributed to the Mo^{6+} state of MoO_3, typical of the Mo–O bond [50]–[52]. The formation of this kind of bond has been reported elsewhere [18], [51], [53], [54], and suggests strong chemical and electronic coupling between the MoS_2 and rGO NSs in the synthesized samples. It shows the existence of Mo oxide state in the MoS_2 due to the presence of oxygen in rGO NSs. In addition, the S 2p region shows two characteristic peaks [Fig. 4(c)] located at 162.0 and 163.3 eV corresponding to S $2p_{3/2}$ and S $2p_{1/2}$, respectively, which can be indexed to Mo–S bonding in MoS_2. The C1s peak [Fig. 4(d)] can be deconvoluted into two peaks, a large peak at 284.6 eV attributed to C–C bonding environment associated with the rGO NSs, and a smaller peak at 285.7 eV attributed to C–O bonding.

TGA was employed to determine the thermal stability of MoS_2 in the rGO–MoS_2 hybrids, and its weight loss curve is shown in Fig. 5. In Fig. 5, it can be observed that TGA of rGO NSs and rGO–MoS_2 hybrids obviously shows two main weight losses. For rGO NSs, the weight loss starts very slowly from room temperature to around 450 °C (~5 wt%), after that its decrease very rapidly and completed by 620 °C (~98 wt%). However, in the case of rGO–MoS_2 hybrids, the initial weight loss was very small from room temperature to 470 °C (~1.4 wt%) and after that fast weight loss was observed up to 740 °C (~15 wt%). These initial weight losses were likely due to the evaporation of surface absorbed water molecules and the presence of an oxygen containing functional groups. The higher weight losses were due to the decomposition and combustion of rGO NSs. For rGO–MoS_2 hybrids, the change represents its thermal decomposition and ~15% weight loss in this temperature range reveals the conversion of MoS_2 to MoO_3 and gaseous SO_2 [55]–[57].

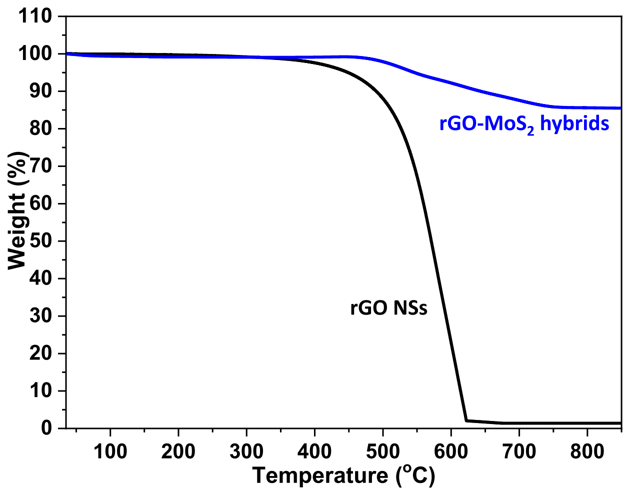

Fig. 5. TGA curve of rGO NSs and rGO–MoS_2 hybrids.

TABLE I

SENSOR RESPONSE FOR DIFFERENT GASES (N_2, O_2, AND NH_2)

Sensor type	Gas	$\Delta U/U$, %	P, mbar	τ, sec	[$\Delta U/U$]/P, % / mbar
Thick film (2 mm)	N_2	-0.13	290	20	- $4.4x10^{-4}$
	O_2	0.34	5.7	50	0.059
	NH_3	0.18	0.48	15	0.38
Thin film (0.01 mm)	O_2	0.15	0.029	10	5.2
	NH_3	0.19	0.008	8	24

Some preliminary results of gas sensing measurements are shown in Table I for both (thick and thin film) sensors, where $\Delta U/U$ is the sensor response (relative change of the voltage after exposure to gases with pressure P), τ is the response time, and $[\Delta U/U]/P$ is the sensitivity. In all cases, the recovery time was considerably larger than the response (rise) time, usually being in the order of hundreds of seconds compared with the rise time of a few tens of seconds. Table I contains the data for different gases N_2, O_2, and NH_3 which has been used for application purposes.

As can be seen, the highest sensitivity is achieved for NH_3vapor, followed by oxygen (which is an order of magnitude lower). Much lower sensitivity was obtained for nonreactive gas N_2. The type of response was also different for nitrogen, when the resistance of the sensing element was reduced upon exposure to the gas. In contrast, during exposure to oxygen and NH_3 vapor, an increase of resistance was detected that may be attributed to the formation of negative ions like O^- during gas interaction with the surface of material resulting in a decrease of measured current [58]. As no gas–solid reaction is expected for nitrogen, the observed small increase of current can be probably attributed to filling the pores by gas making the whole system less resistive. Finally, the sensitivity for NH_3 and O_2 for a thin sensitive rGO–MoS_2 layer (a few parts per million) is about two orders of magnitude higher compared to the thick layer, being approximately inversely proportional to the layer thickness. This finding indicates that in the case of thick sensitive films only the top layers effectively interact with the gas, changing their resistance.

These preliminary results show great potential for the use of thin film rGO–MoS_2 hybrid material for sensing applications. Relatively high sensitivity to gases such as oxygen and NH_3 vapor was achieved at room temperature, while in conventional gas sensors-based, for example, on titanium oxide, temperatures as high as 200 °C–300 °C are usually required to get reasonable sensitivities [58].

IV. CONCLUSION

In summary, we have successfully synthesized rGO–MoS_2 hybrids by *in situ* microwave reduction and exfoliation. Our simple, fast, and low-cost synthesis approach provides a high quality of rGO–MoS_2 hybrids that play a good role in sensing application. Preliminary results with gas sensing (O_2, N_2, and NH_3) show the great potential of a rGO–MoS_2 hybrid material for sensing applications; the highest sensitivity was achieved here for very thin sensitive layers (10 μm thick) at room temperature using a flexible polymer substrate. Further experiments are in progress aiming at the optimization of the gas sensor to achieve enhanced sensitivity and faster response and recovery times. In particular, the use of thinner layers and moderate temperatures up to 100 °C is planned to achieve smaller recovery time and more sensitive detection of gases.

REFERENCES

[1] O. Akhavan, M. Kalaee, Z. S. Alavi, S. M. A. Ghiasi, and A. Esfandiar, "Increasing the antioxidant activity of green tea polyphenols in the presence of iron for the reduction of graphene oxide," *Carbon*, vol. 50, no. 8, pp. 3015–3025, 2012.

[2] P. Salvo *et al.*, "Graphene-based devices for measuring pH," *Sens. Actuators B, Chem.*, vol. 256, pp. 976–991, Mar. 2018.

[3] Y. Niu *et al.*, "MoS_2 graphene fiber based gas sensing devices," *Carbon*, vol. 95, pp. 34–41, Dec. 2015.

[4] S. Basu and P. Bhattacharyya, "Recent developments on graphene and graphene oxide based solid state gas sensors," *Sens. Actuators B, Chem.*, vol. 173, pp. 1–21, Oct. 2012.

[5] F. Yavari and N. Koratkar, "Graphene-based chemical sensors," *J. Phys. Chem. Lett.*, vol. 3, no. 13, pp. 1746–1753, 2012.

[6] Q. He, S. Wu, Z. Yin, and H. Zhang, "Graphene-based electronic sensors," *Chem. Sci.*, vol. 3, no. 6, pp. 1764–1772, 2012.

[7] G. Lu, L. E. Ocola, and J. Chen, "Reduced graphene oxide for room-temperature gas sensors," *Nanotechnology*, vol. 20, no. 44, p. 445502, 2009.

[8] V. Dua *et al.*, "All-organic vapor sensor using inkjet-printed reduced graphene oxide," *Angew. Chem. Int. Ed.*, vol. 49, no. 12, pp. 2154–2157, 2010.

[9] L. J. Cote, R. Cruz-Silva, and J. Huang, "Flash reduction and patterning of graphite oxide and its polymer composite," *J. Amer. Chem. Soc.*, vol. 131, no. 31, pp. 11027–11032, 2009.

[10] W. Li *et al.*, "Reduced graphene oxide electrically contacted graphene sensor for highly sensitive nitric oxide detection," *ACS Nano*, vol. 5, no. 9, pp. 6955–6961, 2011.

[11] M. A. Worsley, P. J. Pauzauskie, T. Y. Olson, J. Biener, J. H. Satcher, Jr., and T. F. Baumann, "Synthesis of graphene aerogel with high electrical conductivity," *J. Amer. Chem. Soc.*, vol. 132, no. 40, pp. 14067–14069, 2010.

[12] M. A. Worsley *et al.*, "Mechanically robust 3D graphene macroassembly with high surface area," *Chem. Commun.*, vol. 48, no. 67, pp. 8428–8430, 2012.

[13] M. A. Worsley *et al.*, "Synthesis and characterization of highly crystalline graphene aerogels," *ACS Nano*, vol. 8, no. 10, pp. 11013–11022, 2014.

[14] F. Schedin *et al.*, "Detection of individual gas molecules adsorbed on graphene," *Nature Mater.*, vol. 6, pp. 652–655, Jul. 2007.

[15] J. D. Fowler, M. J. Allen, V. C. Tung, Y. Yang, R. B. Kaner, and B. H. Weiller, "Practical chemical sensors from chemically derived graphene," *ACS Nano*, vol. 3, no. 2, pp. 301–306, 2009.

[16] T. O. Wehling, K. S. Novoselov, S. V. Morozov, E. E. Vdovin, M. I. Katsnelson, A. K. Geim, and A. I. Lichtenstein, "Molecular doping of graphene," *Nano Lett.*, vol. 8, no. 1, pp. 173–177, Dec. 2008.

[17] A. K. Geim, "Graphene: Status and prospects," *Science*, vol. 324, no. 5934, pp. 1530–1534, Jun. 2009.

[18] H. Long *et al.*, "High surface area MoS_2/graphene hybrid aerogel for ultrasensitive NO_2 detection," *Adv. Funct. Mater.*, vol. 26, no. 28, pp. 5158–5165, 2016.

[19] B. Cho *et al.*, "Charge-transfer-based gas sensing using atomic-layer MoS_2," *Sci. Rep.*, vol. 5, Jan. 2015, Art. no. 8052.

[20] A. Shokri and N. Salami, "Gas sensor based on MoS_2 monolayer," *Sens. Actuators B, Chem.*, vol. 236, pp. 378–385, Nov. 2016.

[21] Y. Liu *et al.*, "Hydrogen gas sensing properties of MoS_2/Si heterojunction," *Sens. Actuators B, Chem.*, vol. 211, pp. 537–543, May 2015.

[22] W. Yang, L. Gan, H. Li, and T. Zhai, "Two-dimensional layered nanomaterials for gas-sensing applications," *Inorganic Chem. Frontiers*, vol. 3, no. 4, pp. 433–451, 2016.

[23] D. Zhang, J. Wu, P. Li, and Y. Cao, "Room-temperature SO_2 gas-sensing properties based on a metal-doped MoS_2 nanoflower: An experimental and density functional theory investigation," *J. Mater. Chem. A*, vol. 5, no. 39, pp. 20666–20677, 2017.

[24] F. K. Perkins, A. L. Friedman, E. Cobas, P. M. Campbell, G. G. Jernigan, and B. T. Jonker, "Chemical vapor sensing with monolayer MoS_2," *Nano Lett.*, vol. 13, no. 2, pp. 668–673, 2013.

[25] W. Di *et al.*, "Construction of MoS_2/Si nanowire array heterojunction for ultrahigh-sensitivity gas sensor," *Nanotechnology*, vol. 28, no. 43, p. 435503, 2017.

[26] Q. He *et al.*, "Fabrication of flexible MoS_2 thin-film transistor arrays for practical gas-sensing applications," *Small*, vol. 8, no. 19, pp. 2994–2999, 2012.

[27] H. Li *et al.*, "Fabrication of single- and multilayer MoS_2 film-based field-effect transistors for sensing NO at room temperature," *Small*, vol. 8, no. 1, pp. 63–67, 2012.

[28] B. Cho *et al.*, "Bifunctional sensing characteristics of chemical vapor deposition synthesized atomic-layered MoS_2," *ACS Appl. Mater. Interfaces*, vol. 7, no. 4, pp. 2952–2959, 2015.

[29] M. Donarelli *et al.*, "Response to NO_2 and other gases of resistive chemically exfoliated MoS_2-based gas sensors," *Sens. Actuators B, Chem.*, vol. 207, pp. 602–613, Feb. 2015.

[30] J.-S. Kim, H.-W. Yoo, H. O. Choi, and H.-T. Jung, "Tunable volatile organic compounds sensor by using thiolated ligand conjugation on MoS_2," *Nano Lett.*, vol. 14, no. 10, pp. 5941–5947, 2014.

[31] K. Lee, R. Gatensby, N. McEvoy, T. Hallam, and G. S. Duesberg, "High-performance sensors based on molybdenum disulfide thin films," *Adv. Mater.*, vol. 25, no. 46, pp. 6699–6702, 2013.

[32] K.-J. Huang, L. Wang, J.-Z. Zhang, and K. Xing, "Synthesis of molybdenum disulfide/carbon aerogel composites for supercapacitors electrode material application," *J. Electroanal. Chem.*, vol. 752, pp. 33–40, Sep. 2015.

[33] K. Chang and W. Chen, "L-cysteine-assisted synthesis of layered MoS_2/graphene composites with excellent electrochemical performances for lithium ion batteries," *ACS Nano*, vol. 5, no. 6, pp. 4720–4728, 2011.

[34] P. T. K. Loan, W. Zhang, C.-T. Lin, K.-H. Wei, L.-J. Li, and C.-H. Chen, "Graphene/MoS_2 heterostructures for ultrasensitive detection of DNA hybridisation," *Adv. Mater.*, vol. 26, no. 28, pp. 4838–4844, 2014.

[35] K. Roy *et al.*, "Graphene–MoS_2 hybrid structures for multifunctional photoresponsive memory devices," *Nat. Nanotech.*, vol. 8, pp. 826–830, Oct. 2013.

[36] Y. Li, H. Wang, L. Xie, Y. Liang, G. Hong, and H. Dai, "MoS_2 nanoparticles grown on graphene: An advanced catalyst for the hydrogen evolution reaction," *J. Amer. Chem. Soc.*, vol. 133, no. 19, pp. 7296–7299, 2011.

[37] M. A. Worsley *et al.*, "Ultralow density, monolithic WS_2, MoS_2, and MoS_2/graphene aerogels," *ACS Nano*, vol. 9, no. 5, pp. 4698–4705, 2015.

[38] B. Radisavljevic, A. Radenovic, J. Brivio, V. Giacometti, and A. Kis, "Single-layer MoS_2 transistors," *Nat. Nanotech.*, vol. 6, pp. 147–150, Jan. 2011.

[39] X. Zheng, J. Xu, K. Yan, H. Wang, Z. Wang, and S. Yang, "Space-confined growth of MoS_2 nanosheets within graphite: The layered hybrid of MoS_2 and graphene as an active catalyst for hydrogen evolution reaction," *Chem. Mater.*, vol. 26, no. 7, pp. 2344–2353, 2014.

[40] B. Cho *et al.*, "Chemical sensing of 2D graphene/MoS_2 heterostructure device," *ACS Appl. Mater. Interfaces*, vol. 7, no. 30, pp. 16775–16780, 2015.

[41] L. Staudenmaier, "Verfahren zur darstellung der graphitsäure," *Berichte Deutschen Chemischen Gesellschaft*, vol. 31, no. 2, pp. 1481–1487, 1898.

[42] R. Kumar *et al.*, "Controlled density of defects assisted perforated structure in reduced graphene oxide nanosheets-palladium hybrids for enhanced ethanol electro-oxidation," *Carbon*, vol. 117, pp. 137–146, Jun. 2017.

[43] A. V. Alaferdov *et al.*, "A wearable, highly stable, strain and bending sensor based on high aspect ratio graphite nanobelts," *Nanotechnology*, vol. 27, no. 37, p. 375501, 2016.

[44] M. Li, X. Cao, S. Zheng, and S. Qi, "Ternary composites RGO/MoS_2@Fe_3O_4: Synthesis and enhanced electromagnetic wave absorbing performance," *J. Mater. Sci., Mater. Electron.*, vol. 28, no. 22, pp. 16802–16812, 2017.

[45] M. Paillet, R. Parret, J.-L. Sauvajol, and P. Colomban, "Graphene and related 2D materials: An overview of the Raman studies," *J. Raman Spectrosc.*, vol. 49, no. 1, pp. 8–12, 2018.

[46] X. Zhang, Q.-H. Tan, J.-B. Wu, W. Shi, and P.-H. Tan, "Review on the Raman spectroscopy of different types of layered materials," *Nanoscale*, vol. 8, no. 12, pp. 6435–6450, 2016.

[47] M. J. Nine, M. A. Cole, L. Johnson, D. N. H. Tran, and D. Losic, "Robust superhydrophobic graphene-based composite coatings with self-cleaning and corrosion barrier properties," *ACS Appl. Mater. Interfaces*, vol. 7, no. 51, pp. 28482–28493, 2015.

[48] A. Dey, A. Chroneos, N. J. S. Braithwaite, R. P. Gandhiraman, and S. Krishnamurthy, "Plasma engineering of graphene," *Appl. Phys. Rev.*, vol. 3, no. 2, p. 021301, 2016.

[49] S. K. Srivastava, B. Kartick, S. Choudhury, and M. Stamm, "Thermally fabricated MoS_2-graphene hybrids as high performance anode in lithium ion battery," *Mater. Chem. Phys.*, vol. 183, pp. 383–391, Nov. 2016.

[50] A. Khademi, R. Azimirad, A. A. Zavarian, and A. Z. Moshfegh, "Growth and field emission study of molybdenum oxide nanostars," *J. Phys. Chem. C*, vol. 113, no. 44, pp. 19298–19304, 2009.

[51] E. G. da Silveira Firmiano *et al.*, "Supercapacitor electrodes obtained by directly bonding 2D MoS_2 on reduced graphene oxide," *Adv. Energy Mater.*, vol. 4, no. 6, p. 1301380, 2014.

[52] Y.-T. Ho *et al.*, "Layered MoS_2 grown on *c*-sapphire by pulsed laser deposition," *Phys. Status Solidi Rapid Res. Lett.*, vol. 9, no. 3, pp. 187–191, 2015.

[53] A. Azcatl *et al.*, "MoS_2 functionalization for ultra-thin atomic layer deposited dielectrics," *Appl. Phys. Lett.*, vol. 104, no. 11, p. 111601, 2014.

[54] H. Nan *et al.*, "Strong photoluminescence enhancement of MoS_2 through defect engineering and oxygen bonding," *ACS Nano*, vol. 8, no. 6, pp. 5738–5745, 2014.

[55] K. C. Wong, X. Lu, J. Cotter, D. T. Eadie, P. C. Wong, and K. A. R. Mitchell, "Surface and friction characterization of MoS_2 and WS_2 third body thin films under simulated wheel/rail rolling–sliding contact," *Wear*, vol. 264, nos. 7–8, pp. 526–534, 2008.

[56] J.-M. Martin, C. Grossiord, K. Varlot, B. Vacher, and J. Igarashi, "Synergistic effects in binary systems of lubricant additives: A chemical hardness approach," *Tribol. Lett.*, vol. 8, no. 4, pp. 193–201, 2000.

[57] C. Liu *et al.*, "Vertical single or few-layer MoS_2 nanosheets rooting into TiO_2 nanofibers for highly efficient photocatalytic hydrogen evolution," *Appl. Catal. B, Environ.*, vol. 164, pp. 1–9, Mar. 2015.

[58] R. V. Gelamo, F. P. Rouxinol, C. Verissimo, A. R. Vaz, M. A. B. de Moraes, and S. A. Moshkalev, "Low-temperature gas and pressure sensor based on multi-wall carbon nanotubes decorated with Ti nanoparticles," *Chem. Phys. Lett.*, vol. 482, nos. 4–6, pp. 302–306, 2009.

Rajesh Kumar received the Ph.D. degree in physics from the Department of Physics, Banaras Hindu University, Varanasi, India.

He is currently a Post-Doctoral Fellow with the Department of Physics, State University of Sao Paulo, Presidente Prudente, Brazil.

Wagner Dias, Jr. received the master's degree in materials science and technology from the State University of Sao Paulo, Presidente Prudente, Brazil, where he is currently pursuing the Ph.D. degree with the Department of Physics.

His current research interests include nanostructured ceramic materials, perovskites, microwave-assisted hydrothermal synthesis, and functional materials.

Rafael J. G. Rubira received the master's degree in materials science and technology from the State University of Sao Paulo, Bauru, Brazil. He is currently pursuing the Ph.D. degree with the Department of Physics, State University of Sao Paulo, Presidente Prudente, Brazil.

Andrei V. Alaferdov received the M.S. degree in nanotechnology in electronics and the Ph.D. degree in physics from the Lobachevsky State University of Nizhni Novgorod, Nizhny Novgorod, Russia, in 2009 and 2016, respectively.

He is currently a Post-Doctoral Fellow with the Center for Semiconductor Components and Nanotechnologies, State University of Campinas, Campinas, Brazil. His current research interests include the synthesis and characterization of carbon nanotubes, graphene, and hybrid structures.

Alfredo R. Vaz received the Ph.D. degree in physics from the Institute of Physics, University of São Paulo, Brazil, in 2004.

Since 2006, he has been with the Center for Semiconductors Components and Nanotechnology, University of Campinas, Campinas, Brazil.

Rajesh K. Singh received the Ph.D. degree in physics from the Department of Physics, Banaras Hindu University, Varanasi, India.

He is currently an Assistant Professor with the School of Physical and Material Sciences, Central University of Himachal Pradesh, Dharamsala, India. His current research interests include hydrogen storage, solid oxide fuel cells, and the synthesis of carbon nanostructures-metal/metal-oxide self-assembly and their applications in different areas.

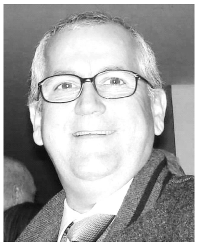

Silvio R. Teixeira received the bachelor's degree in physics, from the University of Brasília, Brasília, Brazil, and the master's degree in nuclear technology and the Ph.D. degree in applied physics from the University of Sao Paulo, Brazil.

He is currently a Professor of physics with the Department of Physics, State University of Sao Paulo, Presidente Prudente, Brazil. His current research interests include clay minerals, solid residues, and functional materials.

Carlos J. L. Constantino received the Ph.D. degree in physics from the Institute of Physics, University of São Paulo, Brazil.

He is currently a Professor of physics with the Department of Physics, State University of Sao Paulo, Presidente Prudente, Brazil. His current research interests include materials science and solid-state physics with emphasis on molecular spectroscopy, fabrication of nanostructured organic films applied to sensors, and mimetic systems of biomembranes.

Stanislav A. Moshkalev (M'99) received the Ph.D. degree in physics from the Ioffe Physical-Technical Institute, St. Petersburg, Russia, in 1984.

He is currently the Director of the Center for Semiconductor Components and Nanotechnology, University of Campinas, Campinas, Brazil. He has authored over 120 articles.

Dr. Moshkalev is a member of Brazilian Physical Society and Brazilian Material Research Society.